Damage-failure transition in titanium alloy Ti-6Al-4V under dwell fatigue loads

Vladimir Oborin, Aleksandr Balakhnin, Oleg Naimark
Institute of Continuous Media Mechanics of Ural branch of RAS, 614013, Perm, Russia
oborin@icmm.ru, http://orcid.org/0000-0003-2836-2073
balakhnin.a@icmm.ru, http://orcid.org/0009-0001-4127-429X
naimark@icmm.ru, http://orcid.org/0000-0001-6537-1177

Yuri Gornostyrev, Vladimir Pushin, Nataliya Kuranova, Dimitrii Rasposienko, Aleksey Svirid, Aleksey Uksusnikov
Institute of Metal Physics, 18, S. Kovalevskaya str., Ekaterinburg 620990, Russia
yug@imp.uran.ru, http://orcid.org/0000-0001-7765-9805
pushin@imp.uran.ru, http://orcid.org/0000-0001-7569-0999
kuranova@imp.uran.ru, http://orcid.org/0000-0002-5330-7909
rasposienko@imp.uran.ru, http://orcid.org/0000-0002-7670-9054
svirid2491@rambler.ru, http://orcid.org/0000-0003-0905-7815
uksusnikov@inbox.ru, http://orcid.org/0000-0003-2551-8968

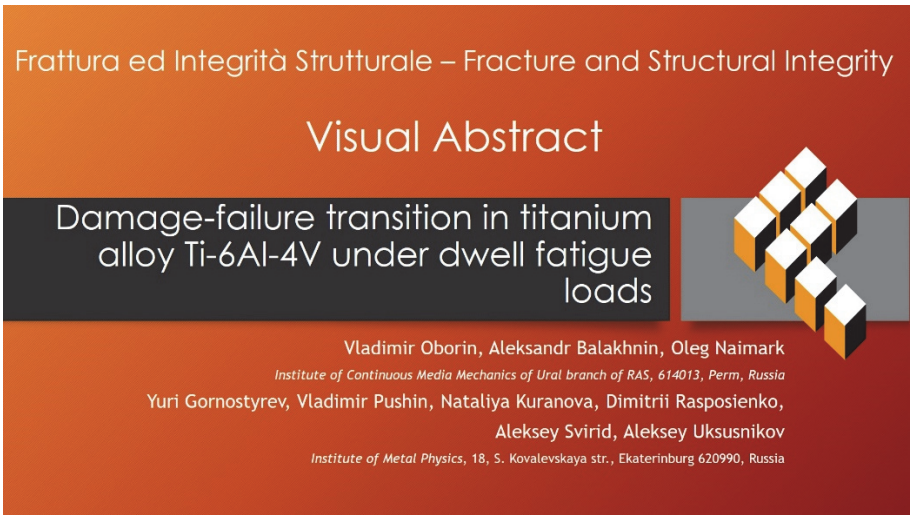

Citation: Oborin, V., Balakhnin, A., Naimark, O., Gornostyrev, Y., Pushin, V., Kuranova, N., Rasposienko, D., Svirid, A., Uksusnikov, A., Damage-failure transition in titanium alloy Ti-6Al-4V under dwell fatigue loads, Frattura ed Integrità Strutturale, 67 (2024) 217-230.

Received: 21.09.2023
Accepted: 01.12.2023
Online first: 06.12.2023
Published: 01.01.2024

KEYWORDS. Fracture, Dwell fatigue, Scaling, Surface morphology, Crack growth kinetics, Microstructure, Texture.

INTRODUCTION

Titanium alloys are widely used for manufacturing the components of gas turbine engines of aircrafts (disk and blade) [1-2], which are subjected complex thermomechanical loading under operating conditions. A significant lifetime reduction occurs in some Ti alloys due to cold dwell fatigue, when the alloys are subjected to fatigue loading and are held at maximum stress level for a period known as "dwell" time during each loading cycle [3]. This is the time when the rate of fatigue damage at ambient temperature increases dramatically in comparison to the conventional fatigue loading [4-6]. The fatigue and cold dwell fatigue lifetimes of aircraft engine components are determined by a variety structural parameters of Ti alloys (composition, microstructure, crystallographic texture). The study of cold dwell fatigue of titanium alloys revealed a significant reduction in fatigue life of gas turbine engines, which served as an impetus to intensive fundamental and applied research [7-8].

The α and transformed β Ti alloys (containing α and β -phases) are used in aerospace applications to create unique properties of flying vehicles at low and moderately high temperature [9]. Structural aspects as the key factors of mechanical behavior were discussed by Bache and Evans [8, 10] and led them to suggest that the process of titanium alloy fracture involves a phenomenon called faceting. The formation of facets and facet micro-cracks occurs on the basal planes of hexagonal close packed (HCP) lattice with orientation of ± 15° with respect to the primary loading direction [9,11-15]. The lifetime under loading conditions, which depends on the faceting process and the facet nucleation, is highly sensitive to the local microstructure as the local grain crystallographic orientations relative to the loading direction, the active slip systems and the grain morphology. The initiation of failure sites (micro-cracks) is associated with the formation of facets and nucleation and coalescence of voids[10, 16]. The faceting process occurs even at room temperature in many Ti-alloys and has the effect of redistribution of stresses from soft grains leading to their increase at some orientated grains. Dwell fatigue in Ti-alloy with a bimodal α/β microstructure was studied by Gerland et al. [17] who found that microcrack nucleation occurs due to the coalescence of voids induced by shear stresses. During cyclic deformation the pile-up of dislocations at the α/β interphase boundaries or α/α grain boundaries are contributed to the kinking and localized shearing of β layers [15, 18]. It was shown that the shearing of β lamellas during dwell-fatigue loading dramatically increases. The size and the number of voids were greater under dwell fatigue loading in comparison with the static creep or normal fatigue conditions. A combination of the cyclic and cold dwell loading with the mechanism of facet nucleation of microcracks has a more damaging effect in Ti-alloy [19].

The lifetime of Ti-alloy is mainly determined by the faceting process, while the microcrack nucleation is dependent on the local microstructural features – the combinations of the local grain crystallographic orientations relative to the macroscale loading direction, the active slip systems, the grain morphology, and the precipitation of secondary phases. The nucleation of fatigue micro-cracks is associated with the slips on the hcp basal planes triggering the faceting process. Clusters of grains (rogue grain combination) with very specific crystallographic orientations relative to the initial loading direction create macrozones or microtextured regions (MTRs). It is an important structural feature of Ti alloys, which plays an important role in fracture development and is actively discussed in recent articles [20-21]. The formation of macrozones is thought to be caused by the selection of variants and the resulting crystallographic orientation relationship between the HCP α (secondary α_s or primary α_p) and BCC β grains during phase transformation under thermomechanical processing conditions. These local texture heterogeneities are of common occurrence in the α and $\alpha + \beta$ (with different ratio of their volume fractions) titanium alloys including Ti-6Al-4V as shown by Sinha [22], Yilun Xu et al. [23], Tympel [3]. It was noted that the effect of MTRs predominates when the fraction of the β– phase is negligible.

A typical load of disks and blades in flight conditions cannot be modeled as a single LCF cycle. The relatively long-term hold or "dwell" at high mean stress during the cruise phase clearly affects the lifetime. Complex LCF loads with cold dwell are more destructive for Ti-alloys, and a possible criterion of their estimation should be associated with the facet nucleation as void nuclei with the following microcrack initiation, crack generation and growth. The elastic-plastic analyses of poly-crystals show that elastic anisotropy in hcp alloys has a significant effect on the local grain-level stresses, accumulated slips, and void nucleation. The length scale effects in the presence of plastic strain gradients are of considerable importance due to an increase in the local grain-level stresses and localization of plastic slips and facet initiation [2, 12,16]. The model of ductile fracture based on the growth and coalescence of voids, which was developed by McClintock [24], Rice and Tracey [25,26], show that porosity in dwell regimes is analogous to creep conditions. However, in the traditional plasticity theory, the stress-strain constitutive relationship of materials is derived from the macroscopic phenomenology of fracture without taking into account the microstructure evolution of materials, which plays a key role in the life-time prediction under dwell fatigue loading conditions[27]. The approach for modeling the behavior of Ti alloys in the dwell fatigue regimes is based on

the results of statistical thermodynamic approach [28,29], which allow us to correlate the collective behavior of defects, the mechanisms of plasticity and defect-induced structural relaxation, and damage-failure transition staging. The key point of this approach is the consideration of the damage-failure transition as a special type of critical phenomena and the structural-scaling transition, when damage develops as a specific phase with characteristic stages, namely, the nucleation of new phase and the phase growth kinetics. In the case of dwell fatigue, the nucleation stage is associated with slip localization, faceting, and void initiation; the phase growth kinetics is related to specific nonlinearity of the free energy release responsible for the staging of damage-failure transition [30-31]. These features are reflected in the statistical phenomenological model of damage-failure transition, which allow us to specify the links of macroscopic material parameters with structural parameters responsible for the influence of microstructure on the structure-sensitive mechanical properties.

This paper presents the results of a comprehensive study of fatigue fracture of titanium alloy under normal low-cyclic and dwell loading conditions, which also includes the microstructure and texture analysis. In this paper, we focus on the role of MTRs in dwell fatigue and consider a Ti-based alloy, in which the fraction of the β phase is very small. Based on the obtained results we develop a damage model of dwell fatigue, the parameters of which can be identified by structural studies.

Al	V	Zr	Si	Fe	C	O	N	H
6.6	4.3	0.021	0.026	0.21	0.009	0.175	0.002	0.0022

Table 1: Chemical composition of Ti-6Al-4V grade (in weight %).

Initial state	Elastic modulus (GPa)	Yield stress (MPa)	Tensile strength (MPa)	Ultimate elongation (%)	Grain size (μm)
CG	115	920	990	13	300
FG after TMT	115	814	950	16	12

Table 2: Quasi-static tensile characteristics of Ti-6Al-4V grade.

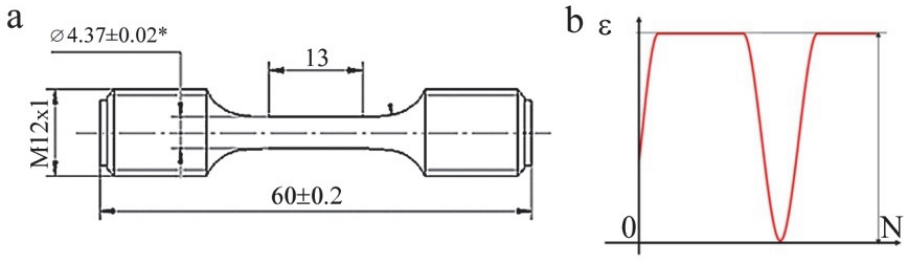

Figure 1: (a) Schematic representation of specimens for low-cycle fatigue test and (b) loading cyclogram (from zero cycle, Rσ=0, with a dwell time of 2, 5, 10 and 20 minutes at maximum load in the cycle) during the LCF resistance test.

MATERIALS AND EXPERIMENTAL CONDITIONS

In this work, we investigate a plate made of Ti-6Al-4V titanium alloy (manufactured VSMPO-AVISMA, Russia). The plate was subjected to thermomechanical treatment (TMT), including rolling at temperatures below the polymorphic $\beta \rightarrow \alpha$ transformation temperature (T_{pt}) until completion of the process. Tab. 1 shows the chemical composition (in weight%) of the alloy. The tensile characteristics of the initial coarse-grained (CG) titanium alloy plates and fine-grained (FG) plates formed after TMT are presented in Tab. 2. Specimens for low-cycle fatigue (LCF) testing were cut from the initial plate along (RD) and across (TD) the hot rolling direction. Fig. 1a shows the geometry of the specimen used in LCF tests (dimensions are indicated in mm). The loading scheme for LCF is shown in Fig. 1b. Test conditions and LCF results for different specimens under normal cyclic and dwell loading conditions are presented in Tab. 3. To study the microstructure, the specimens were cut from the original plate by the electroerosion method, as well as from the heads and the neighborhood of the stretched part of the specimen after low-cycle fatigue testing, and then subjected to mechanical grinding and finishing by ion etching in the PIPS II system. X-ray diffraction (XRD) studies of specimens were carried out in a Brucker D8 Advance diffractometer using CuKα radiation. The scanning electron microscopy (SEM) and fractographic

studies were carried out using the Quanta 200 microscope equipped with Pegasus system and W-cathode, and the Tescan Mira microscope equipped with field thermal emission gun and the Oxford system, which allow making images in different modes (in secondary, SE, and backscattered electrons, EBSD). Chemical element microanalysis, textural and microstructural analyses were performed at the accelerating voltage up to 30 kV. The chemical composition of the specimens was certified using energy dispersive X-ray spectrometry (EDS).

Specimen number	The direction of cutting in relation to the direction of rolling	T, °C	Maximal stress, MPa	Loading	Dwell time, min	Number of cycles (N)
1	along (RD)	20	885	dwell	2	787
2	along (RD)	20	875	dwell	10	1152
3	across (TD)	20	875	dwell	5	288
4	across (TD)	20	885	dwell	2	967
5	across (RD)	20	880	LCF	-	35740
6	across (TD)	20	875	LCF	-	27823

Table 3: Test conditions and LCF results for the specimens of Ti-6Al-4V alloy cut along and across the hot rolling direction.

RESULTS AND DISCUSSIONS

The TMT results in the formation of fine-grained (FG) microstructure in the titanium alloy plate. It has been found that the grains of the HCP α_{2H} phase have a nearly equiaxed shape with an average size of about 12 μm. Fig. 2 a, b shows the grain size distribution of the α phase in colors corresponding to the size groups depicted in the histograms (Fig. 2 c, d). It should be noted that the size distribution of crystallites in the plate is homogeneous and the grains along the rolling direction (RD is slightly elongated.

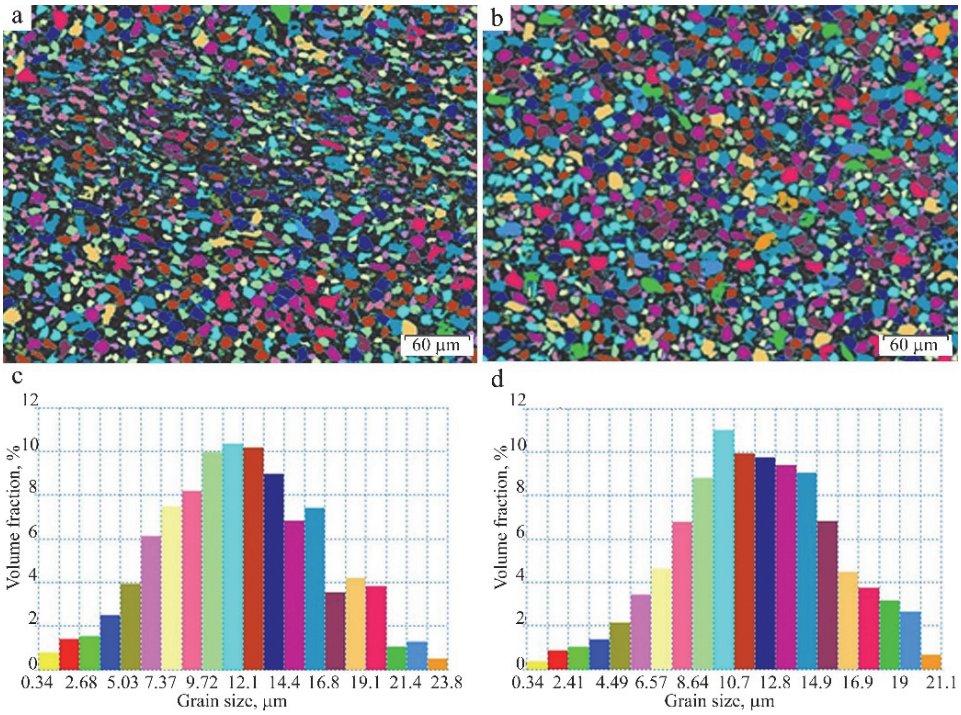

Figure 2: (a-d) The microstructure, histogram of the size distribution of particles of the primary α-phase and their volume fraction (a, c) along (RD) and (b, d) across (TD) of the Ti-6Al-4V alloy specimen

The results of microanalysis of chemical element (Al, Ti, V) distribution near the surface of plate in the initial state of the alloy are shown in Fig. 3. The localization of vanadium atoms along the grain boundaries and a decrease in its content inside the grain is clearly visible.

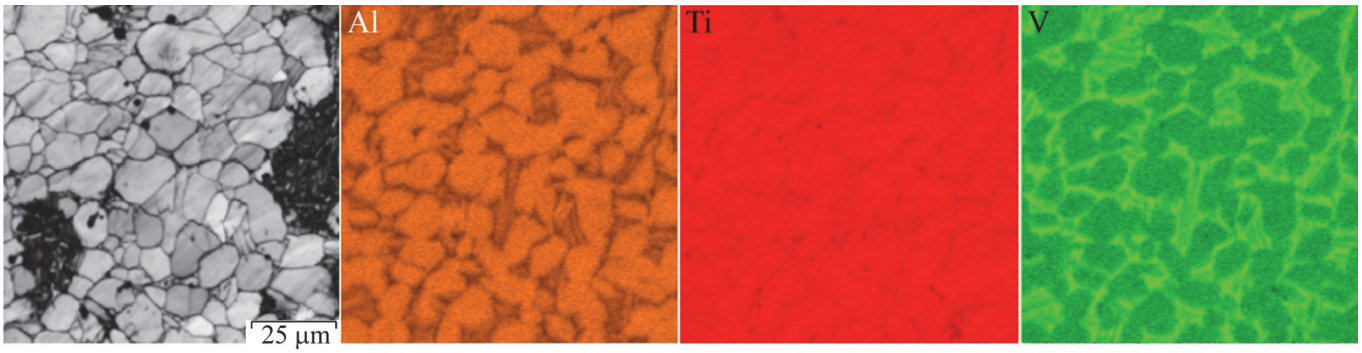

Figure 3: SEM-image of microstructure and mapping by chemical elements in characteristic radiation during energy-dispersive microanalysis of Ti-6Al-4V alloy.

Fig. 4 shows the microstructure as a combination of the EBSD images [32] in three projections: on the rolling plane (with normal ND), as well as on two side faces with normal RD or TD along (RD) and across (TD) the rolling directions. It was found that crystallographic orientations of the α grains alternate from layer to layer in accordance with the change in the color of orientations on the stereographic triangle of the inverse pole figure (IPF) (Fig. 4a). As is seen from Fig. 4a, the orientations of crystals in the basic (0001), prismatic (01$\bar{1}$0) and pyramidal ($\bar{1}$01$\bar{1}$) planes dominate on these faces. The grains of two other orientations dominate on the side faces. The thickness of the textured layers reaches 100-150 μm. The number of α-FG crystals across textured layers is about 5 - 10 grains of close orientation (with scattering up to 10°). The β-phase is practically not observed.

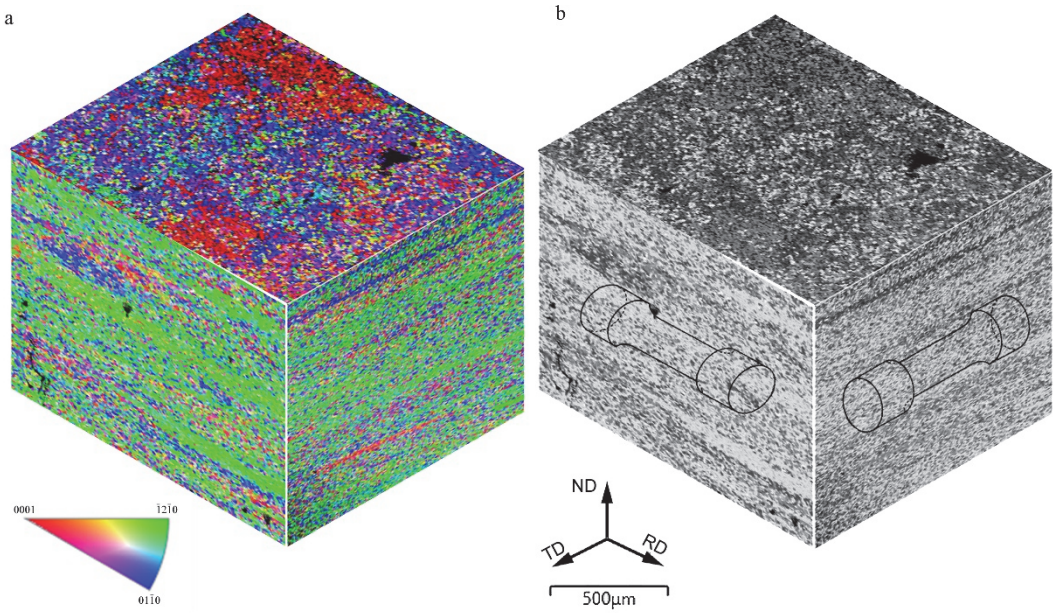

Figure 4: (a) Microstructure of the initial plate of titanium alloy VT6 in three projections on the planes with normal ND (normal direction), RD (rolling direction), TD (transverse direction) and (b) scheme of cutting specimens for LCF.

Fig. 5 shows examples of extended MTR of α-crystals with similar orientation (small-angle misorientation) in the initial state (a, b), as well as on the cross section near the fracture surface after LCF (c) and dwell-LCF (d) tests. There is a significant difference between the structures of the MTRs in the initial state and after fatigue test. The textural perfection of MTRs and

their length increase, reaching few millimeters after dwell LCF (Fig. 5d). On the contrary, the MTRs disintegrate already after normal LCF (Fig. 5c).

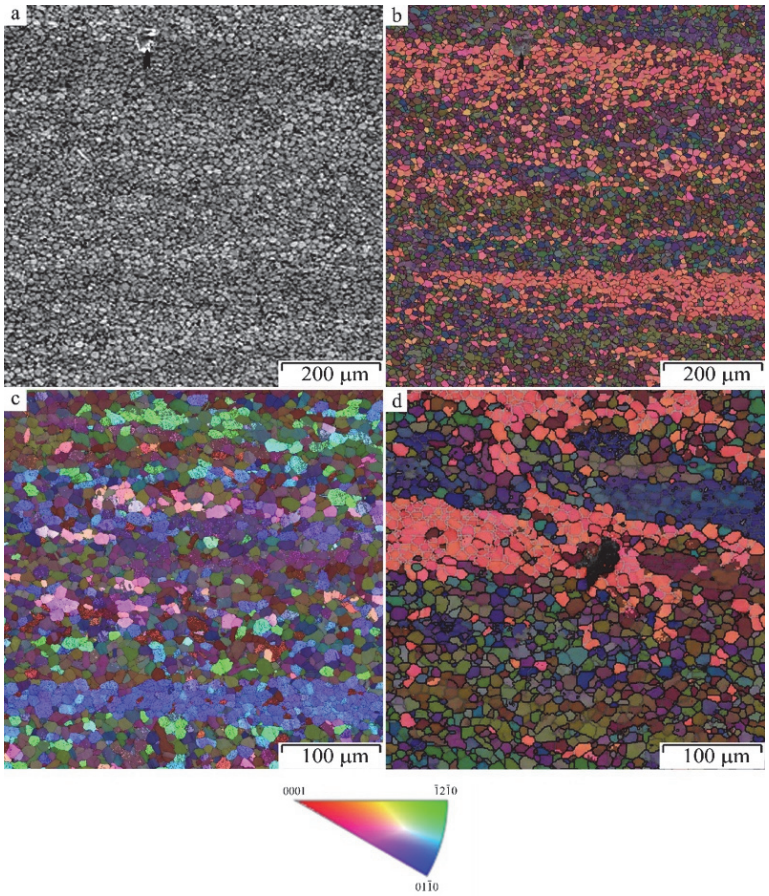

Figure 5: (a) Typical SE and (b-d) EBSD pictures of macrozones (MTR) of α-crystals in the initial state (a, b), after LCF (c) and dwell LCF test (d).

The X-ray diffraction patterns of the specimens corresponding to the initial state of the alloy are shown in Fig. 6. It can be seen that the main Bragg reflections (100, 002, 101 and 110) of the α phase are well pronounced, which is indicative of a strong texture of the specimens. The amount of residual β phase does not exceed 3-5 wt.%. Thus, as mentioned above, the specimen subjected to TMT is almost single-phase with a regular layered distribution of textural crystallographic orientations (with predominance of high-angle 60° and 90° misorientations between MTRs) and the layered morphology is more pronounced for the side faces of the plate (Fig. 4a).

Fig. 7 shows the SEM maps of crystallographic orientation distribution for different poles at the vertices of a stereographic triangle obtained by the EBSD method. The regions of localization of grain orientations (corresponding MTRs) are clearly visible. The coincident crystallographic orientations are depicted in the same color (green, red, or blue). A more detailed orientation distribution of α crystallites in the areas with layered morphology (including MTRs) can be obtained from the maps of distribution of grain microstructure in the Euler orientation angles, which characterize the rotation of the grains until the coincidence with the Z- orientation (Fig. 8).

The details of the microstructure discussed above determine the features of fracture of Ti-6Al-4V alloy specimens.

Typical examples of fractographic patterns after LCF tests are shown in Fig. 9. The fracture surface exhibits a pronounced comb-like topography, apparently reflecting the layered orientation distribution of α crystallites (Fig. 9a). At larger magnification it is clearly seen that the facet pattern of fracture cells dominates, coinciding in size with α-FG crystals and implying the existence of a planar intergranular fracture mechanism along the boundaries of individual α grains (Fig. 9 c, d). This fracture mechanism is characteristic of both types of LCF. The fracture surface of specimens subjected to dwell loading, in contrast to specimens of cyclic tests often exhibits flat extended areas of planar fracture of brittle cleavage along MTRs (Fig. 9 a,b). For larger crystallites, one can observe an undulating moiré contrast, which is expected in the case of sliding

along pyramidal or prismatic crystallographic systems (Fig. 9 d) and is similar in appearance to the contrast in Fig. 9 c and after dwell LCF tests.

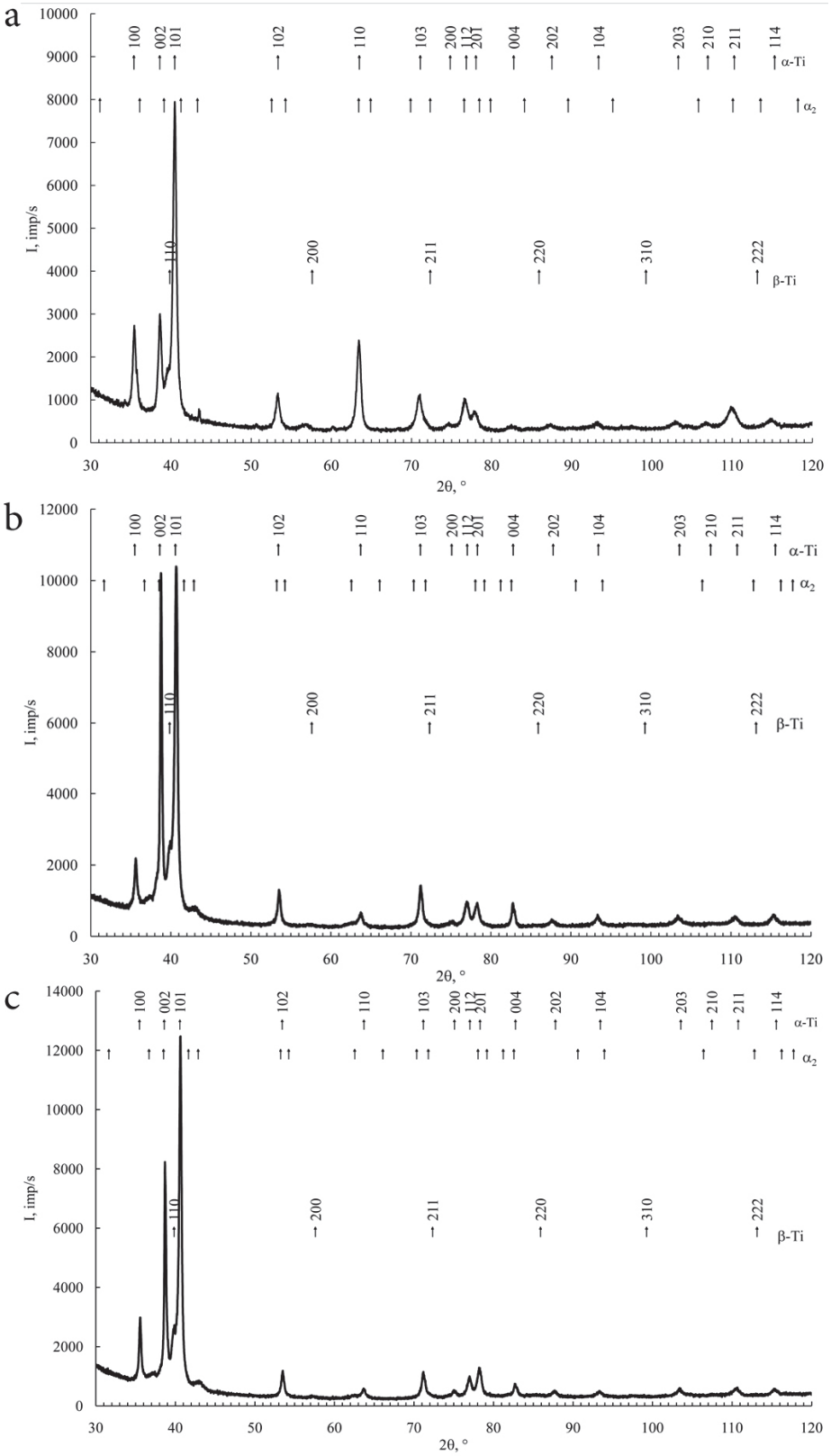

Figure 6: X-ray diffraction patterns of specimens of the original plate of the Ti-6Al-4V alloy, obtained (a) on ND and (b, c) on two side faces (RD and TD) (Fig. 4 a, b).

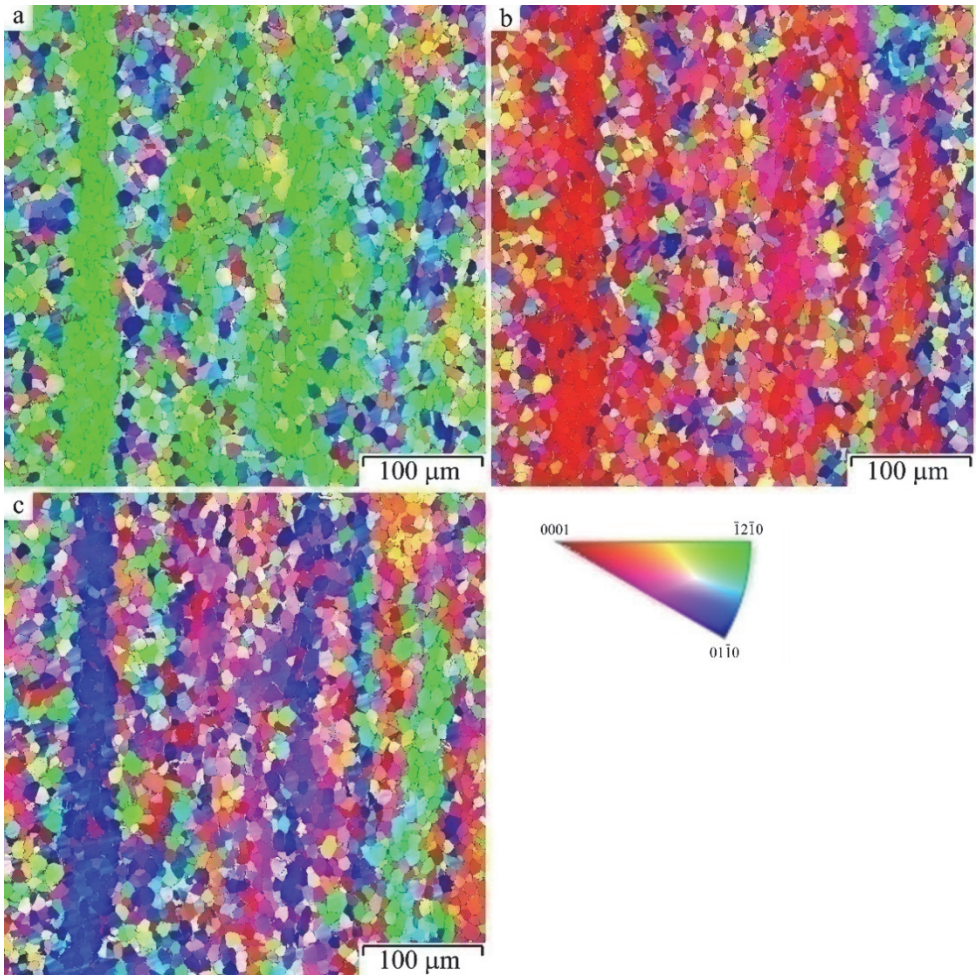

Figure 7: Maps of grain distribution in crystallographic orientations (a - c) across the rolling direction (TD) using reversed pole figures obtained by EBSD.

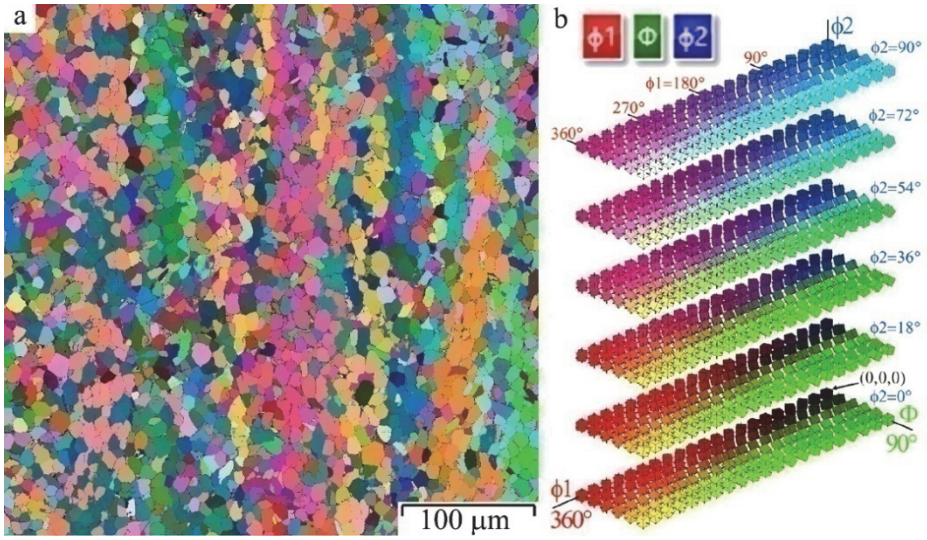

Figure 8: Maps of grain distribution in crystallographic orientations in colors of Euler angles (a) ensuring the rotation of the grain until it coincides with the Z axis (b).

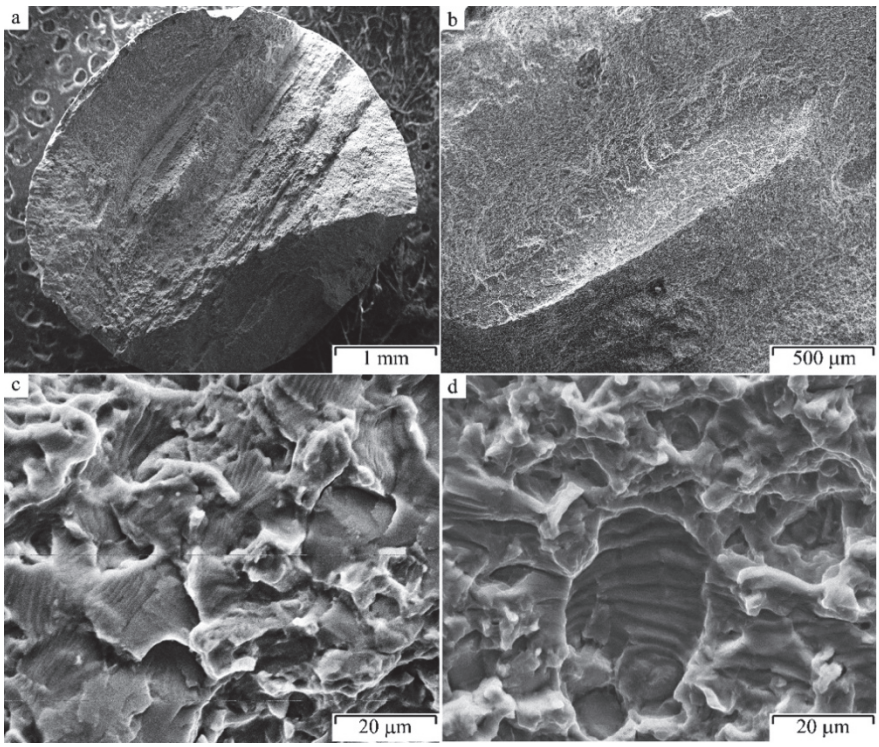

Figure 9: Typical fracture patterns of Ti-6Al-4V alloy specimens after LCF (a-c) dwell or (d) normal cyclic loading.

Thus, the fundamental feature of alloy fracture after dwell LCF can be specified as follows. In addition to the facet mechanism of intergranular fracture along the boundaries of individual α-crystals, there is the mechanism of prematurely flat fracture along MTRs, which reduces the number of LCF cycles by two orders of magnitude (Tab. 3) [3]. A decrease in the number of cycles is explained primarily by the greater stress accumulation and less relaxation possibilities under the dwell conditions in comparison with the usual LCF mode, which results in fracture along MTRs.

CONTINUUM DAMAGE MODEL OF DWELL FATIGUE

This approach focuses on the damage mechanism and damage modeling of titanium alloy in LCF interrupted by a dwell period with stress hold, as well as realization of the damage kinetics due to the plastic flow and the subsequent defect growth in the framework of quasi-brittle scenario governed by the damage-induced free energy release. We consider the conventional phenomenology of damage accumulation due to the plastic flow. The unified phenomenology was proposed by Naimark [28-29]. In these studies, the X-ray small angle in-situ data were used to identify the characteristic features of the damage accumulation in ductile materials: nucleation of numerous voids with the aspect ratio ~1:2 and the progressive increase of concentration during the plastic flow at a relatively stable void volume. It has been presumed that the basic mechanism of the void-induced damage is the formation of the void nuclei due to slip localization. Under plastic deformation the void accumulation is the predominant damage accommodation mechanism in different phases (grains) with specific crystallography. The proposed phenomenological law expressed in the tensor invariant form relates the void-induced strain in the specific volume p to the plastic strain rate invariant ε

$$\frac{\mathrm{d}p_I}{\mathrm{d}t} \sim \alpha \frac{d\varepsilon_I}{\mathrm{d}t} \tag{1}$$

where α is the material parameter reflecting the accommodation of polycrystalline structure to numerous slips due to the void initiation.

The damage kinetics in the dwell period with a stress hold can be associated with free (stored) energy release , which in tensor invariant-based form reads

$$\frac{\mathrm{dp}_I}{\mathrm{dt}} \sim -\gamma \frac{\mathrm{dF}\left(p_I, \sigma_I\right)}{\mathrm{dp}_I} \tag{2}$$

where $F\left(p_I, \sigma_I\right)$ is the free energy of solid with defects in terms of damage (defect- induced strain) and stress σ_I variables in tensor invariant form; γ is the material parameter relating the thermodynamic driving force in solid with defects to the damage kinetics. The damage kinetics in (2) is determined by the non-linearity of the free energy release $\gamma \mathrm{dF} / \mathrm{dp}_I$. The form of free energy was determined [33-34] in the course of statistical thermodynamic description of the collective behavior of defects (microcracks, microshears). It was shown that different forms of metastability of F in terms of the damage parameter (defects induced strain) can be represented in a generalized Ginzburg-Landau form [28] as

$$F\left(p_I, \sigma_I\right) = \frac{1}{2} A\left(1 - \frac{\delta}{\delta_*}\right) \mathrm{p}_I^2 - \frac{1}{4} \mathrm{Bp}_I^4 + \frac{1}{6}\left(1 - \frac{\delta}{\delta_c}\right) \mathrm{Cp}_I^6 - \mathrm{Dp}_I \sigma_I \tag{3}$$

where A, B, C, and D are the material parameters.

The material parameters in Eqns. 1, 2, 3 are specified into two types: kinetic parameters α and thermodynamic parameters *A,B,C*, and *D* that are responsible for the free energy non-linearity (the free energy release due to the damage accumulation). The form of the free energy was established in the course of statistical-thermodynamic description of defects ensemble (microshears, microcracks). This theory revealed two specific types of criticalities in defects ensemble specified by the value of structural-scaling parameter, the current susceptibility of material to the defects, and critical values of this parameters δ_* and δ_c. The first one is due to the formation of collective orientation mode of defects and the second is due to the blow-up damage localization as the crack initiation precursor. The structural-scaling parameters δ_* and δ_c are related to the texture morphology.

This metastability reflects two specific types of criticality of damage-failure transition: the orientation ordering of defect ensemble coordinated by the defect interaction and the external stress, and damage localization on the characteristic length scales as a precursor of the critical crack size.

The parameters δ_* and δ_c are the critical values of the structural-scaling parameter δ responsible for the material structural sensibility to the defect growth. It was shown that this parameter represents the ratio of two characteristic structural scales: the mean inter-defect spacing (defect nuclei) and the mean size of defects. The critical values of δ are responsible for damage orientation ordering, while δ_* and δ_c - for damage localization and crack initiation. The initial material structure susceptibility to damage is determined by the facet and void nucleation stage with the kinetics following Eqn. 1. The material parameter α characterizes the void nucleation kinetics as the accommodation mechanism to plastic slips and depends on α and β phase interaction for localized slips and faceting.

The transformation of voids into microcracks is controlled by a thermodynamic driving force (free energy release) and considered as the natural thermodynamic stage of critical nuclei growth followed by the new phase nucleation. This stage includes two specific kinds of criticality of damage-failure transition at different types of metastability of free energy (3) coordinated by the defect interaction and the external stress: damage in the presence of orientation ordering of the defect ensemble in the range of the structural-scaling parameter δ, and damage localization over the characteristic length scales as a precursor of critical crack size in the range δ.

The damage kinetics in case of complex load history of dwell fatigue includes both types of the damage kinetics obeying the generalized law [28]

$$\frac{\mathrm{dp}_I}{\mathrm{dt}} \sim \alpha \frac{d\varepsilon_I}{\mathrm{dt}} - \gamma \frac{\mathrm{dF}\left(p_I, \sigma_I\right)}{\mathrm{dp}_I} \tag{4}$$

Two damage sources in (4) reflect qualitative different ductile and quasi-brittle mechanisms of damage kinetics in dwell fatigue regimes: void-induced damage as the accommodation mechanism to plastic slips and defect (microcracks, microshears)- induced mechanism of structural relaxation caused by the free energy release.

Eqn. 4 can be reduced qualitatively to the Manson-Coffin law to use the normalization of the damage parameter as the ratio p / p_c, where p_c is the critical value of damage corresponding to the blow-up regime of damage kinetics. Using this

normalization procedure and the following integration over the number of cycle N (instead time) up to N_c (corresponding to p_c), the link of $\alpha\,(d\varepsilon_I/\mathrm{dt})N_c$ and "accumulated" over the range $(0, N_c)$ damage due the free energy release can be established. The power laws for plastic strain rate $(d\varepsilon_I/\mathrm{dt})$ and critical cycles N_c in classical Manson-Coffin law will be replaced in this case into the power law of free energy release on $p/p_c \to 1$.

The tensor invariant form allows accounting for the damage staging associated with the "ductile kinetics" of facet formation due to the slip localization along the maximum shear stress plane, following the void nucleation with the aspect ratio related to the maximum shear stress plane. The void coalescence kinetics governed by the second source term provides a new invariant for the damage parameter p_I, which reflects a new orientation of the damage (microcracks ensemble) mode associated with the tensile stress component.

The duality of damage kinetics mechanisms is the key factor providing different sensitivities of material to the regimes of dwell fatigue. Slip ordering, facet and void kinetics are responsible for stress relaxation during the plastic flow with relatively homogeneous void distribution. This mechanism doesn't dominate in the dwell period governed by the free energy release and results in the damage kinetics with very pronounced spatial-temporal defect localization up to the state of crack nucleation [35].

The inherent link between the faceting with localized slips and damage is related to the thermodynamic origin of void initiation as the accommodation mechanism of dislocation movement over the set of crystallography planes associated with macroscopic stress. The ductile mechanism of damage accumulation can be related with the stage of damage nucleation through the initiation and growth of numerous voids with the mean size specified by the properties of α and β phases of titanium alloys. The dwell period is characterized by the qualitative change in the damage mechanism when the trigger of the damage accumulation is the free energy release and the growth of voids (microcrack) in conditions of a slight change of the crack nucleation sites. The nonlinearity of the free energy release reflects the physical mechanism of void (microcrack) coalescence up to the critical damage localization on the length-scale associated with initiation of critical cracks and their growth according to the Paris crack kinetics. From the viewpoint of general approach to the damage-failure transition kinetics in dwell fatigue there is a need to analyze two stages: (i) ductile damage during LCF with numerous critical voids that originate from the nuclei associated with the facets representing the localized slip area at the α/β interface or α/α grain boundaries; (ii) the growth of the critical voids according to the kinetics of free energy release. Both these mechanisms are represented in the damage evolution equation by the parameters that could be specified according to the structural and mechanical tests. It should be emphasized that the two stages of dwell fatigue involve both mechanisms of damage kinetics described in Eqn. 4 when passing the yield stress during LCF load and stress hold load.

Conclusion

The structure of microtextured regions (MTRs) and their influence on the dwell fatigue behavior of titanium α alloy (Ti-6Al-4V) has been investigated. The attempt was made to specify the dwell fatigue phenomena from the viewpoint of engineering applications, to estimate the role of structural mechanisms responsible for the consequent staging of damage-failure transition as the combination and continuity of ductile and creep kinetics of structure evolution and to define the key aspects of modeling in dwell fatigue regime. The phenomenology of ductile and quasi-brittle failure is discussed taking into account the specific mechanisms of damage kinetics due to the plastic deformation in the conditions of LCF and the characteristic features of the damage scenario related to the free energy release, which occurs in "dwell period" and associated with the creep damage.

The key point of phenomenology of damage-failure transition with regard to the dwell fatigue is a comparative analysis of phenomenological model with statistically based thermodynamic model of collective behavior of solids with defects. The developed concept of modelling of Ti alloys, which is based on the duality of damage kinetics in dwell fatigue loads, allowed us to propose the strategy of structural study, which in prospect can substantiate the relationship between the structural parameters of α/β phases and the phenomenological parameters responsible for different mechanisms of damage accumulation in LCF and stress hold regimes. The structural study was conducted for the specimens cut from the titanium alloy rolling plate in three rolling directions: on the rolling plane (ND), as well as on two side faces along (RD) and across (TD) the rolling directions. The study of the EBSD images allowed us to estimate the initial phase anisotropy, α-phases clusters, grain size distribution for the initial state and on the cross section near the fracture surface after cyclic and dwell LCF tests. This data of structural state of Ti alloy will be used to establish the correlation with mechanical dwell fatigue test

for the specimens cut from different areas of the rolling plate and identification of the material parameters in the damage evolution equation.

Thus far, the relationship between the specific microstructures and dwell fatigue damage has remained mechanistically uncertain, so that the primary goal of this research is to establish a link between the microtextured regions and the dwell fatigue damage, as well as gain insight into the mechanisms of preferential sub-surface facet nucleation under dwell fatigue loading conditions.

To reveal the origin of the spatial scales that determine the fracture kinetics, the study of microstructure and texture of Ti-6Al-4V grade alloys was carried out. We have found that after thermomechanical treatment the plate has practically single-phase structure and is characterized by a layered distribution of fine α grains with minor misorientation within the layers. It can be assumed that such structure arises due to the combined reaction of polymorphic β - α transformation, the globularization and the dynamic recrystallization mechanism occurring during hot TMT, which is accompanied by the mutual size-orientation accommodation of ensembles of α crystals inside and between the layers. The average grain size α of crystals is about 12 μm, and the initial β phase is practically absent (not exceeding 3-5 wt.%). It has been established that the intergranular facet fracture mechanism dominates in fatigue failure during LCF testing. Along with this general failure mechanism, dwell loading of the specimen is associated with premature fracture along flat extended MTRs. The length of MTRs in the longitudinal direction significantly exceeds the size of the α grains, while in the transverse direction it is only few grains (100 – 150 μm). Apparently, this spatial scale plays a crucial role in fracture under dwell fatigue conditions and is responsible for a dramatic reduction of the number of LCF cycles.

AUTHOR CONTRIBUTION

Author contributions are following. Conceptualization: O.B.N. (Oleg B. Naimark), Yu.N.G (Yuri N. Gornostyrev), V.G.P. (Vladimir G. Pushin); methodology V.A.O. (Vladimir A. Oborin), A.N.B. (Alexander N. Balakhnin), N.K. (Nataliya Kuranova), (D.R) Dimitrii Rasposienko, A.S. (Aleksey Svirid), A.U. (Aleksey Uksusnikov); writing-original draft preparation: O.B.N., Yu.N.G., V.G.P.; supervision: O.B.N.

ACKNOWLEDGEMENTS

This research was supported by the Russian Science Foundation (project 21-79-30041), https://rscf.ru/en/project/21-79-30041/ Structural study was performed on the scientific equipment of the Shared Facilities Center of the Mikheev Institute of Metal Physics (Ural Branch, Russian Academy of Sciences).

REFERENCES

[1] Bache, M.R. (2003). A review of dwell sensitive fatigue in titanium alloys: the role of microstructure, texture and operating conditions, Int. J. Fatig., 25, pp. 1079–1087. DOI: 10.1016/S0142-1123(03)00145-2.

[2] Cuddihy, M.A., Stapleton, A., Williams, S., Dunne, F.P.E. (2017). On cold dwell facet fatigue in titanium alloy aero-engine components, Int. J. Fatig., 97, pp. 177–189. DOI: 10.1016/j.ijfatigue.2016.11.034.

[3] Tympel, P.O., Lindley, T.C., Saunders, E.A., Dixon, M. and Dye, D. (2016). Influence of complex LCF and dwell load regimes on fatigue of Ti–6Al–4V, Acta Mater., 103, pp. 77–88. DOI: 10.1016/j.actamat.2015.09.014.

[4] Bache, M., Cope, M., Davies, H., Evans, W. and Harrison, G. (1997). Dwell sensitive fatigue in a near alpha titanium alloy at ambient temperature, Int. J. Fatigue, 19(93), pp. 83–88. DOI: 10.1016/S0142-1123(97)00020-0.

[5] Evans, W.J., Gostelow, C.R. (1979). The effect of hold time on the fatigue properties of a β-processed titanium alloy, Metall. Trans. A, 10, pp. 1837–1846.

[6] Sinha, V., Mills, M.J. and Williams, J.C. (2004) Understanding the contributions of normal-fatigue and static loading to the dwell fatigue in a near-alpha titanium alloy, Metall. Mater. Trans. A, 35(10), pp. 3141–3148.

[7] Rezaei, M., Zarei-Hanzaki, A., Anousheh, A.S., Abedi, H.R., Pahlevani, F., Hossain, R., Sahajwalla, V., Berto, F. (2021) On the damage mechanisms during compressive dwell-fatigue of β-annealed Ti-6242S alloy, Int. J. Fatig., 146, pp.106158. DOI: 10.1016/j.ijfatigue.2021.106158.

[8] Evans, W.J., Bache, M.R. (1994). Dwell-sensitive fatigue under biaxial loads in the near-alpha titanium alloy IMI685, Int. J. Fatig., 16, pp. 443–452. DOI: 10.1016/0142-1123(94)90194-5.
[9] Dunne, F. P. E., Rugg, D. and Walker, A. (2007). Lengthscale-dependent, elastically anisotropic, physically-based hcp crystal plasticity: Application to cold-dwell fatigue in Ti alloys, Int. J. Plast., 23(6), pp. 1061–1083. DOI: 10.1016/j.ijplas.2006.10.013.
[10] Littlewood, P. D. and Wilkinson, A. J. (2012). Local deformation patterns in Ti–6Al–4V under tensile, fatigue and dwell fatigue loading, Int. J. Fatigue, 43, pp. 111–119. DOI: 10.1016/j.ijfatigue.2012.03.001.
[11] Lefranc, P., Doquet, V., Gerland, M. and Sarrazin-Baudoux C. (2008). Nucleation of cracks from shear induced cavities in an α/β titanium alloy in fatigue, room-temperature creep and dwell-fatigue, Acta Mater., 56(16), pp. 4450–4457. DOI: 10.1016/j.actamat.2008.04.060.
[12] Pilchak, A. L. (2013). Fatigue crack growth rates in alpha titanium: Faceted vs. striation growth, Scripta Mater., 68, pp. 277-280. DOI: 10.1016/j.scriptamat.2012.10.041
[13] Song, Z., Hoeppner, D.W. (1989). Size effect on the fatigue behavior of IMI 829 titanium alloy under dwell conditions, Int. J. Fatig., 11, pp. 85–90. DOI: 10.1016/0142-1123(89)90002-9
[14] Sinha, V., Mills, M. J. and Williams, J. C. (2007). Determination of crystallographic orientation of dwell fatigue fracture facets in Ti-6242 alloy, J. Mater. Sci., 42(19). DOI: 10.1007/s10853-006-0252-z.
[15] Sinha, V., Spowart, J. E., Mills, M. J. and Williams, J. C. (2006). Observations on the faceted initiation site in the dwell-fatigue tested Ti-6242 alloy: Crystallographic orientation and size effects, Metall. Mater. Trans. A, 37A(5), pp. 1507–1518.
[16] Dunne, F.P.E. and Rugg, D. (2008). On the mechanisms of fatigue facet nucleation in titanium alloys, Fatigue Fract. Eng. Mater. Struct., 31(11), pp. 949–958. DOI: 10.1111/j.1460-2695.2008.01284.x.
[17] Gerland, M., Lefranc, P., Doquet, V. and Sarrazin-Baudoux, C. (2009). Deformation and damage mechanisms in an α/β 6242 Ti alloy in fatigue, dwell-fatigue and creep at room temperature. Influence of internal hydrogen, Mater. Sci. Eng. A, 507(1–2), pp. 132–143. DOI: 10.1016/j.msea.2008.11.045.
[18] Bache, M.R., Dunne, F.P.E. and Madrigal, C. (2010). Experimental and crystal plasticity studies of deformation and crack nucleation in a titanium alloy, J. Strain Anal. Eng. Des., 45(5), pp. 391–399. DOI: 10.1243/03093247JSA594.
[19] Sinha, V., Mills, M.J. and Williams, J.C. (2004). Understanding the contributions of normal-fatigue and static loading to the dwell fatigue in a near-alpha titanium alloy, Metall. Mater. Trans. A, 35(10), pp. 3141–3148.
[20] Dunne, F.P.E., Walker, A. and Rugg, D. (2007). A systematic study of hcp crystal orientation and morphology effects in polycrystal deformation and fatigue', Proc. R. Soc. Math. Phys. Eng. Sci., 463(2082), pp. 1467–1489. DOI: 10.1098/rspa.2007.1833.
[21] Bache, M.R., Evans, W.J. and Davies, H.M. (1997). Electron back scattered diffraction (EBSD) analysis of quasi-cleavage and hydrogen induced fractures under cyclic and dwell loading in titanium alloys, J. Mater. Sci., 32(13), pp. 3435–3442.
[22] Sinha, V., Mills, M.J. and Williams, J.C. (2006). Crystallography of fracture facets in a near-alpha titanium alloy, 37(6), pp. 2015–2026.
[23] Yilun Xu, Joseph, S., Karamched, P., Fox, K., Rugg, D., Dunne, F.P.E., Dye, D. (2020). Predicting dwell fatigue life in titanium alloys using modelling and experiment, Nature Communications, 11, pp. 5868. DOI: 10.1038/s41467-020-19470-w.
[24] McClintock, F. A. (1968). A Criterion for Ductile Fracture by the Growth of Holes, J. Appl. Mech., 35(2), pp. 363–371. DOI: 10.1115/1.3601204.
[25] Rice, J.R. and Tracey, D.M. (1969). On the ductile enlargement of voids in triaxial stress fields, J. Mech. Phys. Solids, 17, pp. 201-217. DOI: 10.1016/0022-5096(69)90033-7.
[26] Rice, R. (1971). Inelastic constitutive relations for solids: An internal-variable theory and its application to metal plasticity, J. Mech. Phys. Solids, 19(6), pp. 433–455. DOI: 10.1016/0022-5096(71)90010-X.
[27] Muth, A., John, R., Pilchak, A., Kalidindi, S.R., McDowell, D.L. (2021). Analysis of Fatigue Indicator Parameters for Ti-6Al-4V microstructures using extreme value statistics in the transition fatigue regime. Int. J. of Fatigue, 153, pp.106441. DOI: 10.1016/j.ijfatigue.2020.106096.
[28] Naimark, O.B. (2004). Defect Induced Transitions as Mechanisms of Plasticity and Failure in Multifield Cintinua, Advances in Multifield Theories of Continua with Substructure, Capriz, G. and Mariano, P., eds., Boston: Birkhauser, pp. 75–114.
[29] Naimark, O.B. (2003). Collective Properties of Defect Ensembles and Some Nonlinear Problems of Plasticity and Fracture, Phys. Mesomech., 6(4), pp. 39–63. DOI: 10.1134/S1029959917010076.

[30] Naimark, O., Bayandin, Yu., Uvarov ,S., Bannikova, I., Saveleva, N. (2021). Critical Dynamics of Damage-Failure Transition in Wide Range of Load Intensity, Acta Mechanica, 232, p.p. 1943–1959. DOI: 10.1007/s00707-020-02922-1.
[31] Naimark, O., Oborin, V., Bannikov, M., Ledon, D. (2021). Critical Dynamics of Defects and Mechanisms of Damage-Failure Transitions in Fatigue, Materials, 14(10), pp. 2554. DOI: 10.3390/ma14102554.
[32] Britton, T.B., Birosca, S., Preuss, M. and Wilkinson, A.J. (2010). Electron backscatter diffraction study of dislocation content of a macrozone in hot-rolled Ti–6Al–4V alloy, Scr. Mater., 62(9), pp. 639–642. DOI: 10.1016/j.scriptamat.2010.01.010
[33] Lataillade, J.-L. and Naimark, O.B. (2004). Mesoscopic and Nonlinear Aspects of Dynamic and Fatigue Failure (Experimental and Theoretical Results), Phys. Mesomech., 7(3–4), pp. 47–58.
[34] Naimark, O. (2016). Energy release rate and criticality of multiscale defects kinetics, Int. J. Fracture, 202, pp. 271–279. DOI: 10.1007/s10704-016-0161-3.
[35] Froustey, C., Naimark, O., Bannikov, M., and Oborin, V. (2010). Microstructure Scaling Properties and Fatigue Resistance of Pre-strained Aluminium Alloys (Part 1: AleCu Alloy), Eur. J. Mech. A. Solid, 29, pp. 1008–1014. DOI: 10.1016/j.euromechsol.2010.07.005.